minerals

MDPI

Article

Analysis of the Selective Flotation of Elemental Gold from Pyrite Using Diisobutyl Monothiophosphate

Weiping Liu [1,2,3,*], Jan Dean Miller [1,4], Wei Sun [1,2,3] and Yuehua Hu [1,2,3]

1 School of Minerals Processing and Bioengineering, Central South University, Changsha 410083, China
2 Hunan International Joint Research Center for Efficient and Clean Utilization of Critical Metal Mineral Resources, Central South University, Changsha 410083, China
3 Key Laboratory of Hunan Province for Clean and Efficient Utilization of Strategic Calcium-Containing Mineral Resource, Center South University, Changsha 410083, China
4 Department of Materials Science & Engineering, University of Utah, Salt Lake City, UT 84112, USA
* Correspondence: wliu.met@csu.edu.cn

Abstract: The gold contained in copper ores is an important resource for the gold industry. In some cases, elemental gold is present and can be recovered by selective flotation. It has been reported that the gold grade and recovery can be increased, without sacrificing the copper recovery, by replacing AERO 3477 (diisobutyl dithiophosphate (DTP)) with AERO 7249 (mixture of diisobutyl monothiophosphate (MTP) and diisobutyl dithiophosphate (DTP)) as the main collector. The fundamental understanding of the improvement in selectivity with the addition of MTP in the flotation of elemental gold from pyrite is limited and is the subject of this paper. In this regard, the hydrophobicity and selectivity of DTP and MTP in the flotation of pyrite and gold are compared and discussed. Density functional theory (DFT) was used to examine the electron density, reactivity, highest occupied molecular orbital (HOMO), and lowest unoccupied molecular orbital (LUMO) of the MTP and DTP collectors. The interaction energies for the adsorption of MTP and DTP from fresh pyrite, oxidized pyrite and gold surfaces were calculated and discussed with respect to the experimental results reported in the literature. Molecular dynamics simulation (MDS) was used to examine the adsorption state of MTP and DTP on the pyrite (100) and Au (111) surfaces.

Keywords: gold; pyrite; dithiophosphate; monothiophosphate; DFT; MDS; flotation

Citation: Liu, W.; Miller, J.D.; Sun, W.; Hu, Y. Analysis of the Selective Flotation of Elemental Gold from Pyrite Using Diisobutyl Monothiophosphate. *Minerals* **2022**, *12*, 1310. https://doi.org/10.3390/min12101310

Academic Editor: Jan Zawala

Received: 25 September 2022
Accepted: 14 October 2022
Published: 17 October 2022

1. Introduction

Gold, associated with the base metal sulfides in the earth's crust, in some cases, occurs in the elemental state or as an alloy. For example, such gold is associated with chalcopyrite and is recovered together with the chalcopyrite in the flotation concentrate. However, a small amount of elemental gold is floated as individual particles, and a selective collector is needed to improve the elemental gold flotation recovery.

Cyanide, xanthate and dithiophosphate ligands react with gold to form gold complexes. Cyanide is the most popular ligand for the dissolution of gold from ores into an aqueous solution due to the high stability of the gold cyanide complex when compared to xanthate and dithiophosphate [1–6]. Nevertheless, xanthate and dithiophosphates are commonly used as collectors in the flotation of gold and PGMs (platinum group metals) from gangue minerals. If the collector-mineral complex has great stability with the valuable minerals and gangue minerals at the same time, then the collector exhibits lower selectivity in the flotation of the valuable mineral from the gangue minerals [7]. In the case of liberated noble metals, such as gold, from the sulfide minerals in the ore, a selective collector against the sulfide minerals has technical and economic advantages [7]. For example, minor amounts of elemental gold are present in the Grasberg ore in Indonesia where the selective flotation of elemental gold against pyrite improves gold recovery and grade in the Grasberg mine [8].

Monothiophosphate has the functional group of P(=S)O by the replacement of the S atom with the O atom when compared to the functional group of P(=S)S for dithiophosphate. This small change in chemical structure for the thiophosphate collector creates a remarkable difference in selectivity for the flotation of gold from sulfide minerals in mildly alkaline pH conditions [3,6,9]. Isoamyl dialkyl dithiophosphate increased the gold surface sessile drop contact angle from 44 to 96°, and achieved a greater recovery of coarse native gold by flash flotation when compared to dithiocarbamate [10]. Monothiophosphate was found to adsorb preferentially on the precious metal surface in the presence of large amounts of sulfide minerals in alkaline pH [2,9]. Dicresyl monothiophosphate was commercially used for selective gold flotation at the Sonora Mining Corporation in California [7]. At the Grasberg mine in Indonesia, the gold grade and recovery were increased by 3.37 g/t and 4.5%, respectively, without sacrificing the copper recovery by the replacement of AERO 3477 (diisobutyl dithiophosphate (DTP)) with AERO 7249 (diisobutyl monothiophosphate (MTP) and diisobutyl dithiophosphate (DTP)) as the main collector. The fundamental understanding of the improved selectivity in the flotation of elemental gold from pyrite using MTP has not been established and is the subject of this paper.

To explain the higher selectivity with the addition of MTP in the flotation of gold from pyrite when compared to using only DTP, the adsorption and hydrophobic surface states were evaluated for ideal mineral surfaces and are discussed. Density functional theory (DFT) was used to examine the collector and its adsorption mechanism at the pyrite and gold surfaces. DFT includes, but is not limited to, the electron density, reactivity, highest occupied molecular orbital (HOMO), and lowest unoccupied molecular orbital (LUMO) of the MTP and DTP collectors, and the interaction energies for the adsorption of MTP and DTP at the pyrite and gold surfaces. Molecular dynamics simulation (MDS) was used to examine the adsorption states and interfacial water structure for MTP and DTP on the pyrite (100) and Au (111) surfaces. It is expected that the above results will improve the fundamental understanding of improved gold recovery at Grasberg and should be helpful in the collector design for improved gold grade and recovery.

2. Computational Methods

2.1. Density Functional Theory Calculations

The thiophosphate collectors, DTP and MTP, were dissolved in aqueous solutions; thus, the chemical structures and reactivity were influenced by the extent of dissolution [11,12]. The pK_a values of dithiophosphate and monothiophosphate are commonly less than 6 [13,14]. The flotation of pyrite and gold is typically carried out at pH values above 6. Therefore, the DTP and MTP anion states were used in the molecular dynamics simulations.

The molecular structures for DTP and MTP were calculated by the Gaussian 09 program [15] using a geometry optimization model at the HF/6-31G(D) level as shown in Figure 1. The highest occupied molecular orbital (HOMO), lowest unoccupied molecular orbital (LUMO), and electrostatic potential (ESP) charges were also obtained by density functional theory calculations.

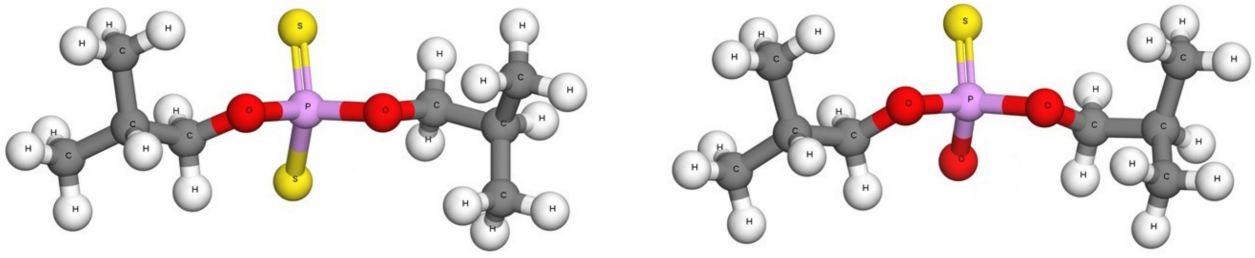

(**a**) (**b**)

Figure 1. Chemical structures of DTP (**a**) and MTP (**b**). White: hydrogen; grey: carbon; red: oxygen; pink: phosphorus; yellow: sulfur.

2.2. Molecular Dynamics Simulations

The molecular dynamics simulations were conducted using Amber 14 [16]. The total energy in MDSs using a classic force field includes the coulombic (electrostatic) energy, the short-range energy (van der Waals energy term), the bond stretch energy, and the angle bend energy. The rigidly extended simple point charge (SPC/E) water model [17] was used to represent the aqueous phase [18]. The crystal lattice parameters for pyrite [19] and gold [20] were from the American Mineralogist Crystal Structure Database. The pyrite (100) surface [21] and gold (111) surface [22] were used for the molecular dynamics simulations. The visual molecular dynamics (VMD) graphics tool [23] was used for the configuration of the collector and mineral surfaces. NVT (moles (N), volume (V), and temperature (T)) together with Hoover's thermostat were used. The integration of the particle motion was evaluated by the leap-frog method with a time step of 1 fs (femtosecond). The electrostatic interactions were represented by the Ewald sum. A final 0.5 ns (nanosecond) simulation was analyzed after a 1.5 ns equilibration period. Detailed principles and procedures for molecular dynamics simulations have been described in a previous paper [24]. The mineral surface relaxation in the molecular dynamics simulations created an additional net-dipole moment and subsequent response of the interfacial water molecules [25]. In this regard, the frozen (fixed) mineral phase was used. The composition and intermolecular potential parameters are presented in Tables 1 and 2. The Gaussian calculated charge for DTP and MTP are shown in Tables 3 and 4.

The Quickstep package of the CP2K program [26] was used to build the optimized Au (111), pyrite (100), and oxidized pyrite (100) structures. The DZVPMOLOPT-SR-GTH shorter range basis set [27] and PBE correlation functional [28] were used in our DFT quantum chemical calculations. The detailed procedure is described in a previous paper [29]. The optimized crystal structures were further expanded for the molecular dynamics simulations.

Table 1. The composition and number of molecules in each system.

	Number of Molecules			
	DTP Anion	**MTP Anion**	**Na^+**	**H_2O**
Au (111)	4		4	1500
Au (111)		4	4	1500
Pyrite (100)	4		4	1500
Pyrite (100)		4	4	1500
Oxidized pyrite (100)	4		4	1500
Oxidized pyrite (100)		4	4	1500

Table 2. The intermolecular potential parameters.

Species	**Charge (e)**	**ε (kcal/mol)**	**r (Å)**	**Reference**
Sodium	1.000	0.5216	3.2282	[30]
Gold	0.000	0.7713	3.0722	[31]
DTP/MTP sulfur		0.3976	4.9929	[31]
DTP/MTP carbon		0.1050	3.8510	[32]
DTP/MTP oxygen		0.6000	3.5000	[32]
DTP/MTP hydrogen		0.4400	2.8860	[32]
DTP/MTP phosphorus		0.3050	4.1470	[32]
Iron in pyrite	0.1476	0.013	2.912	[29]
Sulfur in pyrite	−0.0738	0.274	4.035	[29]
Hydroxyl iron	3	0.013	2.912	[29]
Hydroxyl oxygen	−1.3167	0.152	1.640	[29]
Hydroxyl hydrogen	0.3167	0.000	1.000	[29]
Water oxygen	−0.8476	0.1554	3.1659	[24]
Water hydrogen	0.4238	0	0	[24]

Table 3. Gaussian calculated charge parameters for the DTP anion.

Atom Name	Charge [e]	ATOM NAME	Charge [e]
C	−0.308024	H	−0.048001
C	0.259923	H	−0.020404
C	−0.121701	H	0.002665
C	0.244112	H	0.036149
O	−0.363683	H	0.027715
P	0.422311	H	0.000690
S	−0.599064	H	−0.063874
O	−0.399608	H	−0.070167
C	0.577682	H	0.034316
C	−0.208288	H	0.034618
C	0.157111	H	−0.024317
C	−0.262471	H	−0.027061
S	−0.612446	H	0.067007
H	0.054270	H	0.041720
H	0.056026	H	0.057503
H	0.055289		

Table 4. Gaussian calculated charge parameters for the MTP anion.

Atom Name	Charge [e]	Atom Name	Charge [e]
C	−0.120813	H	−0.007819
C	0.092001	H	−0.007729
C	−0.061733	H	0.010884
C	0.128130	H	0.035472
O	−0.288417	H	0.033271
P	0.766768	H	−0.037141
S	−0.711774	H	0.017794
O	−0.461511	H	0.046481
C	0.397599	H	0.099193
C	−0.373952	H	−0.057805
C	0.304642	H	−0.035487
C	−0.278982	H	0.044973
H	0.019189	H	0.033950
H	0.001636	H	0.081821
H	0.048181	H	−0.680835
H	−0.037984		

2.3. Analysis Methods

The density profiles and atomic densities in the z-axis were used to examine the distribution of the molecules as a function of distance from the mineral surface [33]. The equation for the atomic density follows:

$$\rho_z = \frac{N(Z - 0.5\Delta Z,\ Z + 0.5\Delta Z) \times M}{\Delta Z \times S} \quad (1)$$

$N(Z - 0.5\Delta Z,\ Z + 0.5\Delta Z)$ is the average atom number appearing in the duration of $(Z - 0.5\Delta Z,\ Z + 0.5\Delta Z)$ (ΔZ = 0.01) from the mineral surface. M and S are the atom mass and the basal surface area, respectively.

The diffusion coefficients (D) were derived using the following equation [24]:

$$D = \frac{1}{6N_a} \lim_{t \to \infty} \sum_{i=1}^{N_a} \langle [r_i(t) - r_i(0)]^2 \rangle \quad (2)$$

where N_a is the number of diffusive atoms in the simulation cell; $r_i(0)$ and $r_i(t)$ are the mass center positions of the solutes at the time of origin and t, respectively.

The mineral surface-collector interaction energy, ΔE, was computed using the density functional theory method:

$$\Delta E = E_{complex} - \left(E_{mineral\ surface} + E_{collector}\right) \quad (3)$$

where $E_{complex}$, $E_{mineral\ surface}$, and $E_{collector}$ are the energies of the optimized mineral surface-collector complex, mineral surface, and collector, such as DTP or MTP, respectively. Smaller values of the interaction energy, ΔE, indicate stronger interactions between the mineral surface and the collector [24].

3. Results

The improved selectivity of MTP was observed in the flotation of gold from pyrite, and its mechanism was examined by comparison of density functional theory calculations with the results for DTP. The adsorption states of DTP and MTP on the gold, fresh pyrite, and oxidized pyrite surfaces were examined by molecular dynamics simulations and are discussed together with contact angle and flotation experiment results.

3.1. Analysis of Flotation Results

DTP was observed to float gold and pyrite simultaneously [8]. The flotation difference between gold and pyrite was only around 15 to 35% as a function of pH using DTP [34]. As for MTP, the remarkable flotation difference of 80% between pyrite and gold was found in the alkaline pH region from pH 6 to pH 9 [8,9]; The flotation recovery of pyrite with MTP decreased as a function of pH, a phenomenon also observed in other sulfide mineral flotation systems [8]. In this regard, MTP was preferentially adsorbed on the gold surface without competition from pyrite [9] when compared to the case of DTP.

The laboratory flotation comparison was carried out using AERO 3477 and AERO 7249 at the Grasberg mine, as shown in Table 5. The gold recovery increased from 82.54 to 83.56% at a 95% confidence level with AERO 7249, while the copper recovery was almost the same.

Table 5. Comparison of laboratory flotation performance between AERO 3477 and AERO 7249 [8].

	Recovery, %	
	Cu	**Au**
AERO 3477	87.74	82.54
AERO 7249	87.84	83.56

Plant flotation data from the Grasberg mine using AERO 3477 and AERO 7249 are shown in Table 6. The strong correlation between copper and gold recovery observed was because the majority of gold was associated with chalcopyrite. The gold grade and recovery were increased from 27.80 g/t and 73.73% to 31.17 g/t and 77.81% by using AERO 7249 instead of AERO 3477.

The laboratory and plant flotation results show that gold grade and recovery were improved using AERO 7249 without significantly sacrificing Cu grade and Cu recovery for the Grasberg ore. AERO 7249 was also found to be the best collector in the flotation of gold for the Cadia Hill deposit, Australia [3]. MTP was reported to provide excellent selective recovery of gold, silver, and platinum group metals in froth flotation processes conducted under alkaline conditions [35]. To examine the chemical structure impact on the reactivity and flotation selectivity, density functional theory was used to analyze the DTP and MTP collectors, as discussed in the following sections.

Table 6. The average value of plant data from April 1995 to March 1997 [8].

		AERO 3477	AERO 7249
Feed	% Cu	1.29	1.36
	Au(g/t)	1.35	1.55
Concentrate	% Cu	30.45	29.79
	Au(g/t)	27.80	31.17
Grind size	% + 212 μm	33.29	33.05
Recovery	Copper	84.60	84.30
	Gold	73.73	77.81
Au recovery/Cu recovery ratio		0.871	0.923

3.2. Density Functional Theory Analysis

The chemical reactivity of a collector was determined by the atomic charges of specific atoms, the highest occupied molecular orbital (HOMO), and the lowest unoccupied molecular orbital (LUMO) [36]. The HOMO orbitals evaluate the chemical reactivity and the electron-donating ability, while the LUMO orbitals represent the electron-accepting capacity and the size of the chelating ring formed during the chemical reaction. A higher HOMO or a lower LUMO indicates a stronger electron-donating or electron-accepting ability, respectively [24]. The specific atomic charge in the functional group also contributes significantly to the electron-donating capacity of the collector molecule and to the electrostatic interaction at the mineral surfaces.

The MTP group, P(=S)O, is obtained by the replacement of the S atom with the O atom from the DTP group, P(=S)S. The collector reactivity, which was determined by the molecular orbitals and atomic charges, was significantly changed due to the replacement of the donor atom of S in DTP. In the computational chemistry analysis, the electrostatic potential (ESP) charges and molecular orbitals information were derived using semi-empirical [37] or ab initio methods [38,39]. The optimized structures, ESP charges, and molecular orbitals for DTP and MTP are shown in Figure 2 and Table 7.

Table 7. Theoretical HOMO, LUMO, $\Delta E_{|HOMO\text{-}LUMO|}$ and ESP charge of a polar functional group.

Species	HOMO, a.u.	LUMO, a.u.	$\Delta E_{\|HOMO\text{-}LUMO\|}$, a.u.	ESP Charge of –P = S-S/O	ESP Charge of Reactive Atoms
DTP	−0.1453	0.3244	0.4697	−0.85	−1.18
MTP	−0.1492	0.3285	0.4776	−0.65	−1.39

MTP has a weaker electron-donating and accepting ability according to its lower HOMO of −0.1492 and higher LUMO of 0.3285 when compared to DTP as shown in Table 7. Furthermore, the ESP charge value of 0.85 for –P=S-S in DTP is higher than the case of 0.65 for –P=S-O in MTP, which confirmed that MTP has limited donor ability and as such, a lower reactivity when compared to DTP. However, the reactive atoms' charge value of 1.39 for =S and -O in MTP is higher than 1.18 for =S and –S in DTP, which means the reactive atoms in MTP have a higher electron density capacity or greater donor ability when compared to DTP. In this regard, MTP shows good collecting power toward gold and excellent selectivity against the pyrite, which agrees with the improved gold recovery for the Grasberg ore [8]. In a similar analysis reported in the literature, a short-chain amine collector [40] and a short-chain phosphate collector [24] with lower collecting ability were also observed to have better selectivity, due to the stronger electron-donating ability of the reactive atoms in the polar functional group. To examine the superior selectivity of MTP over DTP in the flotation of elemental gold from pyrite, molecular dynamics simulations

were used to examine the collector adsorption status at the mineral surface, as discussed in the following section.

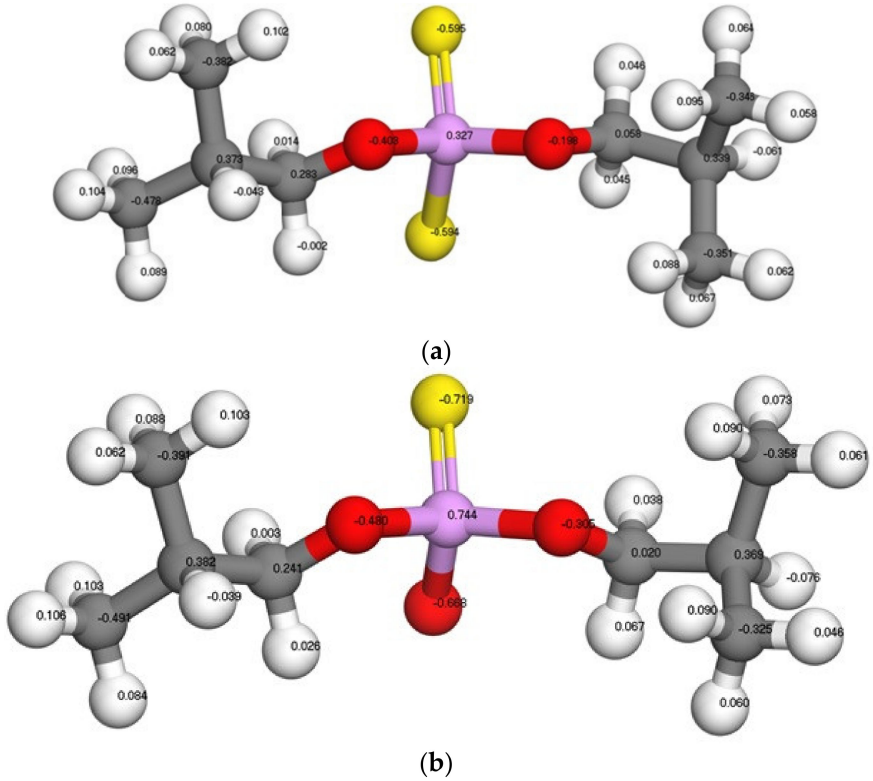

Figure 2. ESP charges of DTP (**a**) and MTP (**b**). White: hydrogen; grey: carbon; red: oxygen; pink: phosphorus; yellow: sulfur.

3.3. Molecular Dynamics Simulations Analysis

The adsorption states of DTP and MTP collectors on Au (111) and pyrite (100) surfaces were examined by molecular dynamics simulations as shown in Figure 3a–d.

DTP and MTP collectors were adsorbed at the Au (111) surface after 1 ns of molecular dynamics simulation, as shown in Figure 3a,b. This phenomenon agrees with the experimental results. The molecular dynamics simulation results and experimental sessile drop contact angle results for the gold surface covered with DTP were 75 and 72°, respectively [41]. Surface-enhanced Raman spectroscopy (SERS) results indicated that DTP was bonded to the gold electrode surfaces through the two S atoms [42]. IR reflectance spectra results suggest that MTP is only physisorbed on the gold surface [9]. As shown in Figure 3a, DTP was adsorbed on the gold surface by S and H atoms, while MTP primarily depended on H atoms, as shown in Figure 3b.

Oxidation of pyrite occurs in these flotation systems and a more hydrophilic surface is created [29]. To evaluate the impact of surface oxidation on pyrite, the adsorption of DTP and MTP was examined both on pure pyrite and oxidized pyrite surfaces. The adsorption of MTP and DTP on pure and oxidized pyrite surfaces, as shown in Figure 3c–f, was mainly by Fe-S bonding, which is the same as the density functional theory calculation result [43]. However, the majority of DTP and MTP collectors were adsorbed on the pure pyrite surface, which contradicts the fact that MTP has superior recovery in the flotation of gold from pyrite. In contrast, the adsorption phenomenon was different on the oxidized pyrite, as shown in Figure 3e,f. All the DTP collector was still adsorbed on the oxidized pyrite surface while only about 40% of the MTP collector was adsorbed on the oxidized pyrite surface. In this regard, the oxidation of the pyrite surface explains the selective flotation of gold from pyrite using MTP. Normally the collector with greater stability with minerals has relatively weak selectivity in the flotation. For example, if collector type A has greater

stability with the minerals than collector type B, then collector type A has weaker selectivity than collector B in the flotation of valuable minerals from gangue minerals. As shown in Figure 3a,c,e, DTP exhibited strong adsorption affinity and adsorbed on almost all the surfaces of gold, pyrite, and oxidized pyrite, which explains the limited selectivity of DTP in the flotation of gold from pyrite.

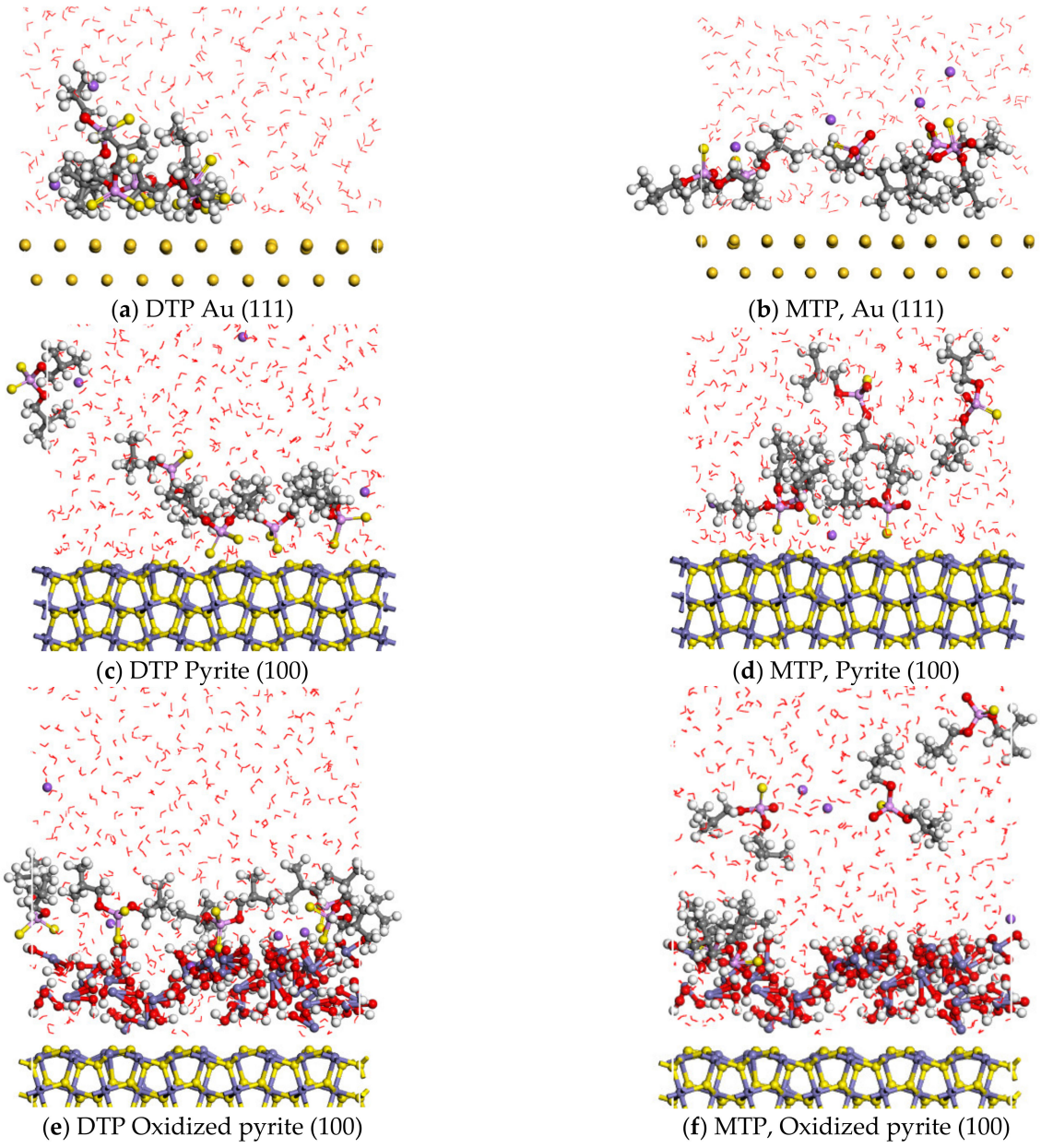

Figure 3. Interfacial behavior of DTP and MTP at the Au (111) surface (**a**,**b**), pyrite (100) surface (**c**,**d**), and oxidized pyrite (100) surface (**e**,**f**). Reagent: white: hydrogen; grey: carbon; red: oxygen; pink: phosphorus; yellow: sulfur. $Fe(OH)_3$: dark grey: iron; white: hydrogen; red: oxygen. Pyrite: yellow: sulfur; purple: iron. Gold: dark yellow: Au.

As shown in Figure 4a,b, both DTP and MTP excluded water from the gold and pyrite surfaces, since the relative number densities of the water in the cases of the DTP and MTP solutions were significantly lower than for pure water at the gold, pyrite and oxidized pyrite surfaces. The relative number densities of water in the presence of DTP and MTP were almost the same on both the gold and pyrite surfaces, which is in accord with the collector adsorption phenomenon on the gold and pyrite surfaces as shown in Figure 3a–d.

As for the oxidized pyrite surface in Figure 4c, the relative number densities of water decreased in the presence of DTP and MTP, as expected. However, DTP had an even lower relative number density of water when compared to MTP, starting at 36 angstroms from the mineral surface, which indicated DTP excluded more water from the oxidized pyrite surface and thus had stronger adsorption and greater hydrophobicity on the oxidized pyrite surface. In this regard, DTP adsorbed not only on gold but also on the pyrite and oxidized pyrite surface, thereby limiting the selective flotation of gold from pyrite. In contrast, MTP excluded a lesser amount of water from the oxidized surface and thereby caused lower hydrophobicity on the oxidized pyrite surface. In the meantime, MTP completely adsorbed on the gold surface and thus superior selectivity was observed in the flotation of gold from pyrite using MTP.

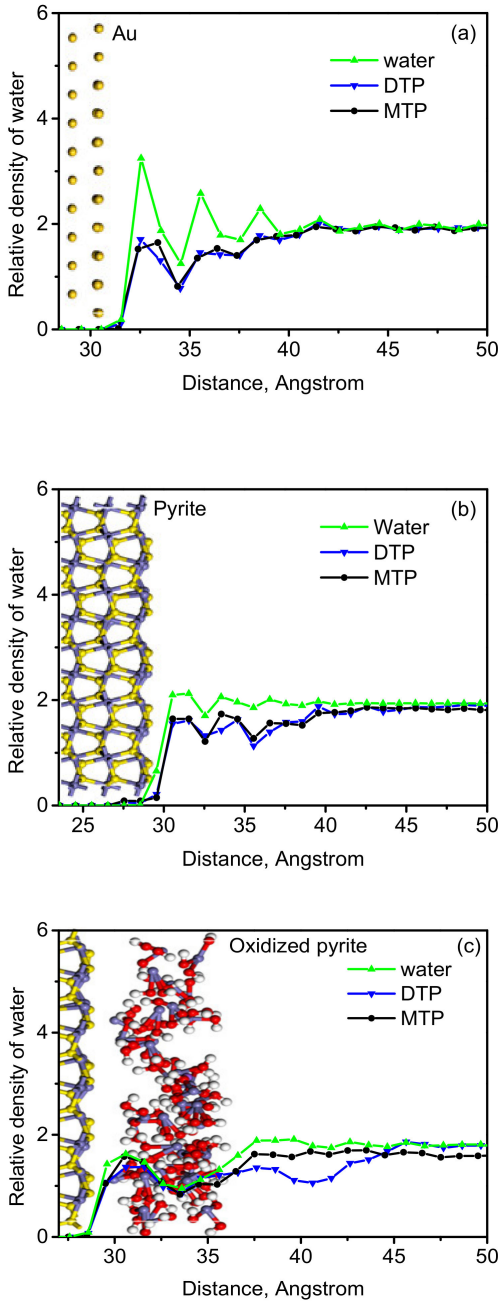

Figure 4. Relative number density distribution of water along the normal to the Au (111) (**a**), pyrite (100) (**b**), and oxidized pyrite (100) (**c**) surfaces with and without DTP/MTP. $Fe(OH)_3$: dark grey: iron; white: hydrogen; red: oxygen. Pyrite: yellow: sulfur; purple: iron. Gold: dark yellow: Au.

The relative number density of atoms from DTP and MTP along the normal to the gold, pure pyrite, and oxidized pyrite surfaces are presented in Figure 5. The peaks of the S atom and H atom from DTP were closer to the gold surface when compared to other atoms as shown in Figure 5a, which agreed with the S atom bonding at the gold surface by surface-enhanced Raman spectroscopy [42]. As for the adsorption of MTP at the gold surface, H and C atoms were the closest atoms, which confirmed that the main adsorption mechanism between MTP and the gold surface was physisorption. The closest atoms to the pure pyrite and oxidized pyrite surfaces were S atoms, as shown in Figure 5c–f. The relative number density of atoms from DTP and MTP were almost the same on the pure pyrite surface, while the relative number density of MTP atoms was less than half of the relative number density of DTP on the oxidized pyrite surface. This observation confirmed that MTP has a lower adsorption affinity on the oxidized pyrite surface when compared to the case of DTP. In this regard, MTP has superior selectivity when compared to DTP in the flotation of gold from pyrite.

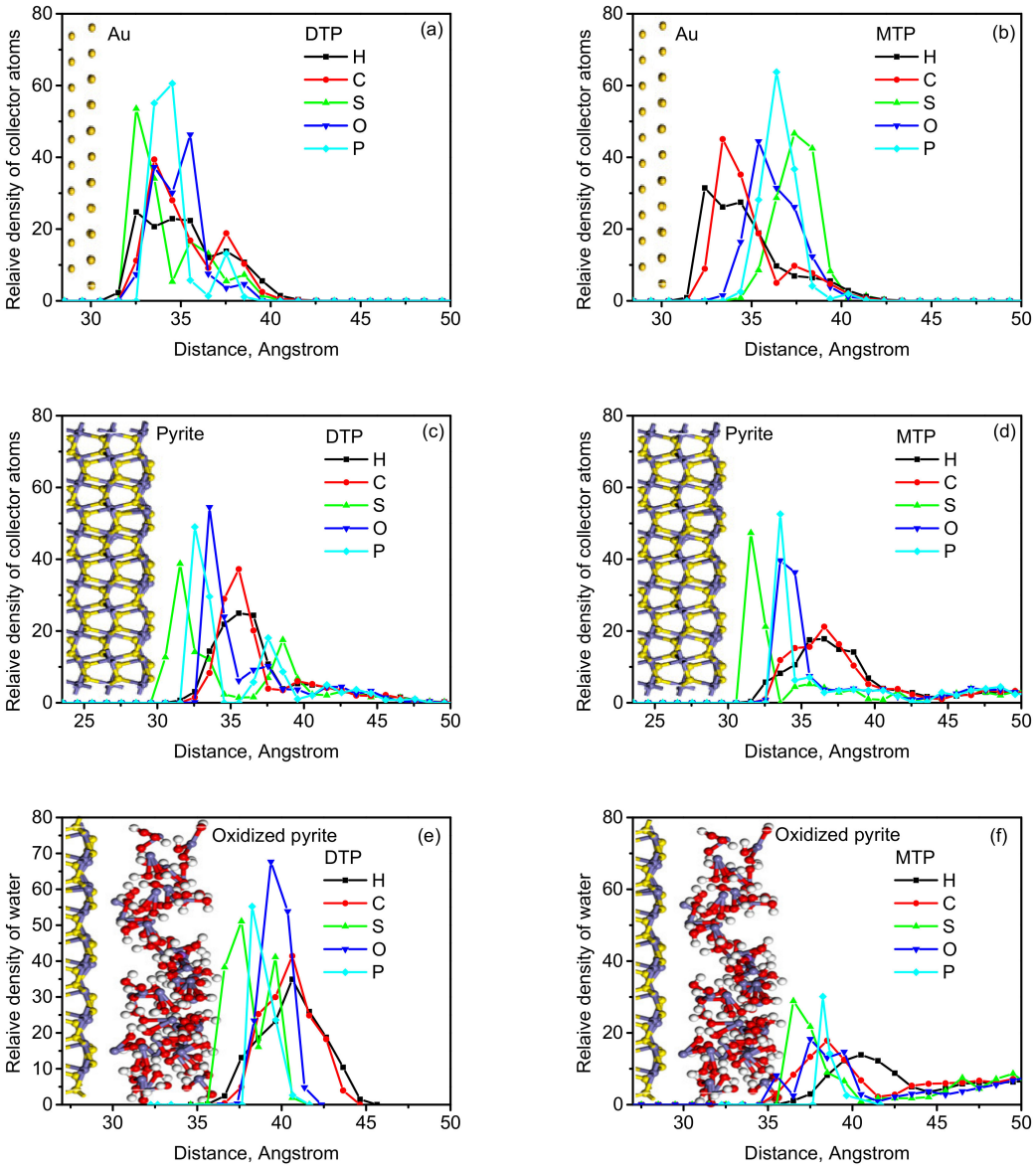

Figure 5. Relative number density distribution of selected atoms from DTP and MTP along the normal to the Au (111) surface (**a**,**b**), pyrite (100) surface (**c**,**d**), and oxidized pyrite (100) surface (**e**,**f**). $Fe(OH)_3$: dark grey: iron; white: hydrogen; red: oxygen. Pyrite: yellow: sulfur; purple: iron. Gold: dark yellow: Au.

Mean square displacement and diffusion coefficients (D) were used to examine the movement of the collector as a function of time in each system. Since DTP and MTP have almost the same chemical structure, the mean square displacement and diffusion coefficients (D) can be indicators for the adsorbed collector at mineral surfaces. Lower mean square displacement and diffusion coefficient (D) values represent a stable/immobile collector at the mineral surface, and accordingly, strong adsorption [44]. A lower mean square displacement of DTP was observed when compared to MTP, as shown in Figure 6, which showed that DTP had a stronger adsorption affinity at almost all of the selected mineral surfaces. A difference in mean square displacement between DTP and MTP was observed for the gold surface. MTP had a higher diffusion coefficient of 17.80×10^{-5} cm^2/s when compared to 3.95×10^{-5} cm^2/s for DTP, providing further indication of the lower adsorption affinity of MTP on the gold surface. The biggest difference in mean square displacement between DTP and MTP was observed on the oxidized pyrite surface compared to the pure pyrite surface, as shown in Figure 6b,c. At the pure pyrite surface, MTP and DTP had diffusion coefficients of 4.62×10^{-6} cm^2/s and 2.54×10^{-6} cm^2/s, respectively. As for the oxidized pyrite surface, MTP and DTP had diffusion coefficients of 32.65×10^{-6} cm^2/s and 0.33×10^{-6} cm^2/s, respectively. The significant difference in mean square displacement between MTP and DTP agreed with the corresponding adsorption states at the oxidized pyrite surface, and showed that little MTP collector was adsorbed at the oxidized pyrite surface, thereby resulting in high selectivity in the flotation of gold from pyrite.

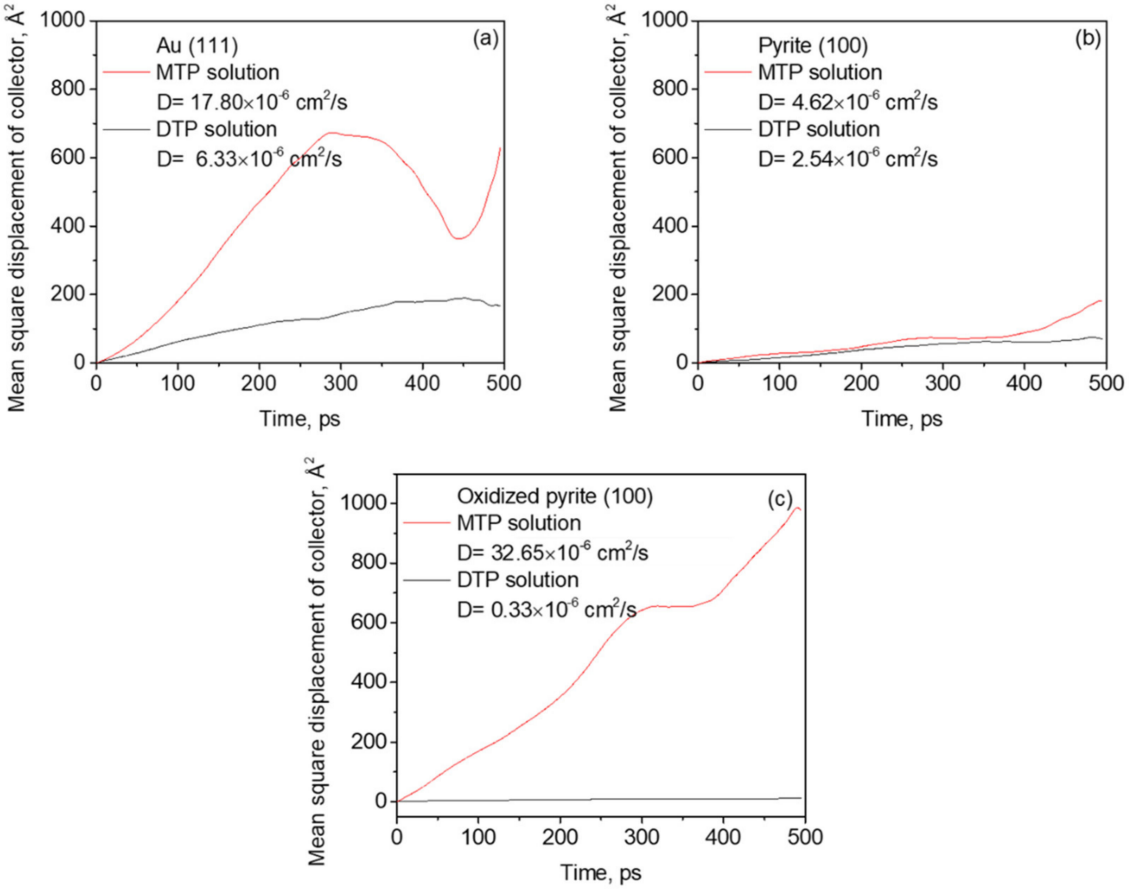

Figure 6. Mean square displacement of DTP/MTP on Au (111) (**a**), pyrite (100) (**b**), oxidized pyrite (100) (**c**) surfaces.

3.4. Interaction Energy

The interaction energies of MTP and DTP at the Au (111), pyrite (100), and oxidized pyrite (100) surfaces are plotted in Figure 7. More negative interaction energy indicates stronger adsorption occurred between the collector and the mineral surface. All the inter-

action energy results for DTP on the specific mineral surfaces were lower than for MTP, which agreed with the flotation and collector analysis results, and indicated that DTP had a stronger reaction when compared to MTP. The interaction energy differences between MTP and DTP on Au (111) and pyrite (100) were 1 kJ/mol and 3 kJ/mol, respectively. This small difference agreed with the adsorption states, as shown in Figure 3, where both MTP and DTP were adsorbed at the gold and pure pyrite surfaces. The interaction energy difference for MTP and DTP on the oxidized pyrite surface was about 17 kJ/mol. This big difference further confirmed that DTP completely adsorbed while only a minor amount of MTP adsorbed on the oxidized pyrite surface. In this regard, MTP provides superior selectivity when compared to DTP in the flotation of gold from pyrite.

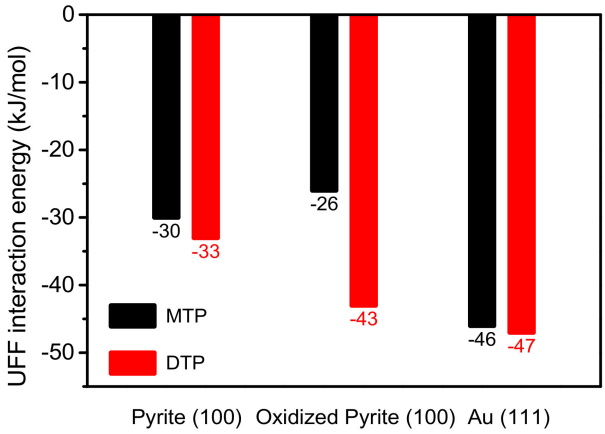

Figure 7. UFF interaction energy of MTP and DTP on Au (111), pyrite (100) and oxidized pyrite (100).

4. Discussion

A selective collector in the flotation of elemental gold from sulfide minerals improves both gold grade and recovery. The typical collector, such as DTP, floats gold and pyrite simultaneously. In contrast, greater selectivity of MTP in the flotation of gold from pyrite was observed from micro flotation and plant flotation results. In this regard, the impact of collector chemical structure on adsorption was examined by density functional theory calculations, which showed that MTP had a good reacting ability toward gold and excellent selectivity against oxidized pyrite. The adsorption states of DTP and MTP on gold, pyrite and oxidized pyrite surfaces were also examined and compared. The molecular dynamics simulation results indicated that DTP had a greater adsorption affinity toward the mineral surfaces when compared to MTP. DTP and MTP collectors were completely adsorbed on the gold and fresh pyrite surfaces. Most of the MTP collectors did not adsorb at the oxidized pyrite surface while DTP was still completely adsorbed at the oxidized pyrite surface. In this regard, the oxidized pyrite surface explains the high selectivity of MTP in the flotation of gold from pyrite. The oxidized pyrite surface also accounts for the selective flotation of gold from pyrite using potassium amyl xanthate [45].

5. Conclusions

To improve the fundamental understanding of surface chemistry in the flotation of elemental gold from sulfide minerals using thiophosphate collectors, density functional theory and molecular dynamics simulations were used to examine the reactivity and adsorption states of DTP and MTP on gold, pyrite, and oxidized pyrite surfaces. The experimental and simulation results indicated that DTP had a greater adsorption affinity toward these mineral surfaces. MTP has effective collecting power for gold and excellent selectivity against oxidized pyrite. The oxidation of pyrite explains the greater selectivity of MTP in the flotation of gold from pyrite.

Conclusions at this time include the following points:

1. Collector analysis showed that MTP has a lower head group charge and less reactivity. However, the reactive atoms of =S and -O in MTP have better electron-donating ability compared to the case of =S and –S for DTP. In this regard, MTP possesses effective collecting power for gold and excellent selectivity against pyrite.
2. The molecular dynamics simulation results indicated that DTP has a greater adsorption affinity at the mineral surfaces when compared to MTP. Furthermore, DTP is adsorbed on gold, pyrite, and oxidized pyrite surfaces, which is in accord with the limited selectivity of DTP in the flotation of gold from pyrite.
3. Both DTP and MTP collectors are completely adsorbed on the gold and fresh pyrite surfaces. Most of the MTP collectors did not adsorb on the oxidized pyrite surface while DTP still completely adsorbed on the oxidized pyrite surface. In this regard, the oxidized pyrite surface contributes to the high selectivity of MTP in the flotation of gold from pyrite.

Author Contributions: Conceptualization, W.L. and J.D.M.; methodology, W.L.; software, W.L.; validation, W.L. and J.D.M.; formal analysis, W.L.; investigation, W.L.; resources, W.S., Y.H. and J.D.M.; data curation, W.L. and J.D.M.; writing—original draft preparation, W.L.; writing—review and editing, W.L. and J.D.M.; visualization, W.L.; supervision, J.D.M.; project administration, J.D.M.; funding acquisition, J.D.M. All authors have read and agreed to the published version of the manuscript.

Funding: Funding for this research by the Division of Chemical Sciences, Geosciences, and Biosciences, Office of Basic Energy Sciences of the U.S. Department of Energy through Grant No. DE-FG03-93ER14315 and the International Precious Metal Institute are gratefully acknowledged.

Data Availability Statement: Data is available based on request.

Acknowledgments: The Gaussian calculations and molecular dynamics simulations were enabled by the Center for High-Performance Computing at the University of Utah. The authors would like to thank Dorrie Spurlock for her assistance in the preparation of the manuscript.

Conflicts of Interest: The authors declare no conflict of interest.

References

1. Cotton, F.A.; Wilkinson, G. *Advanced Inorganic Chemistry*; Wiley: New York, NY, USA, 1998.
2. Nagaraj, D.R. The chemistry and application of chelating or complexing agents in minerals separations. In *Reagents in Mineral Technology*; Somasundaran, P., Moudgil, B., Eds.; Marcel Dekker, Inc.: New York, NY, USA, 1988; pp. 257–334.
3. Forrest, K.; Yan, D.; Dunne, R. Optimisation of gold recovery by selective gold flotation for copper-gold-pyrite ores. *Miner. Eng.* **2001**, *14*, 227–241. [CrossRef]
4. Güler, T.; Hiçyilmaz, C.; Gökağaç, G.; Ekmeçi, Z. Adsorption of dithiophosphate and dithiophosphinate on chalcopyrite. *Miner. Eng.* **2006**, *19*, 62–71. [CrossRef]
5. Larsson, A.-C.; Ivanov, A.V.; Antzutkin, O.N.; Forsling, W. A ^{31}P CP/MAS NMR study of PbS surface O,O′-dialkyldithiophosphate lead (II) complexes. *J. Colloid Interface Sci.* **2008**, *327*, 370–376. [CrossRef] [PubMed]
6. Nagaraj, D.R.; Ravishankar, S.A. Flotation reagents—A critical overview from an industry perspective. In *Froth Flotation: A Century of Innovation*; Society for Mining, Metallurgy, and Exploration: Littleton, CO, USA, 2007; pp. 375–424.
7. Hansen, C.; Killey, L. Selective gold flotation at Sonora Mining's Jamestown concentrator using Aero 5688 promoter. *Min. Met. Process.* **1990**, *7*, 180–184. [CrossRef]
8. Hartati, F.; Mular, M.; Stewart, A.; Gorken, A. Increased gold recovery at PT Freeport Indonesia using Aero 7249 Promoter. In *6th Mill Operators' Conference*; Australasian Institute of Mining and Metallurgy: Melbourne, Australia, 1997; pp. 165–168.
9. Nagaraj, D.R.; Brinen, J.; Farinato, R.; Lee, J. A study of interaction of dicresyl monothiophophate with noble metals by electrochemical and spectroscopic methods. In Proceedings of the SME Annual Meeting, Denver, CO, USA, 26 February–1 March 1991; pp. 91–181.
10. Bustamante-Rúa, M.O.; Najanjo-Gómez, D.M.; Daza-Aragón, A.J.; Bustamante-Baena, P.; Osorio-Botero, J.D. Flash flotation of free coarse gold usingdithiophosphate and dithiocarbamate as a replacement for traditional amalgamation. *Dyna* **2018**, *85*, 163–170. [CrossRef]
11. Field, M.J.; Bash, P.A.; Karplus, M. A combined quantum mechanical and molecular mechanical potential for molecular dy-namics simulations. *J. Comput. Chem.* **1990**, *11*, 700–733. [CrossRef]
12. Tapia, O.; Bertrán, J. *Solvent Effects and Chemical Reactivity*; Springer: Berlin/Heidelberg, Germany, 1996.
13. Alimarin, I.P.; Tat'yana, V.R.; Ivanov, V.M. Extraction with thio and dithio phosphorus acids. *Russ. Chem. Rev.* **1989**, *58*, 863. [CrossRef]

14. Sole, K.C.; Hiskey, J.B. Solvent extraction characteristics of thiosubstituted organophosphinic acid extractants. *Hydrometallurgy* **1992**, *30*, 345–365. [CrossRef]
15. Frisch, M.J.; Trucks, G.W.; Schlegel, H.B.; Scuseria, G.E.; Robb, M.A.; Cheeseman, J.R.; Scalmani, G.; Barone, V.; Mennucci, B.; Petersson, G.A.; et al. *Gaussian 09*; Gaussian, Inc.: Wallingford, CT, USA, 2009.
16. Case, D.A.; Babin, V.; Berryman, J.T.; Betz, R.M.; Cai, Q.; Cerutti, D.S., III; Darden, T.A.; Duke, R.E.; Gohlke, H.; Götz, A.W.; et al. *AMBER 14*; University of California: San Francisco, CA, USA, 2014.
17. Mahoney, M.W.; Jorgensen, W.L. A five-site model for liquid water and the reproduction of the density anomaly by rigid, nonpolarizable potential functions. *J. Chem. Phys.* **2000**, *112*, 8910. [CrossRef]
18. Berendsen, H.J.C.; Grigera, J.R.; Straatsma, T.P. The missing term in effective pair potentials. *J. Phys. Chem.* **1987**, *91*, 6269–6271. [CrossRef]
19. Ramsdell, L.S. *The Crystal Structure of Some Metallic Sulfides*; University of Michigan: Ann Arbor, MI, USA, 1925.
20. Jette, E.R.; Foote, F. Precision determination of lattice constants. *J. Chem. Phys.* **1935**, *3*, 605–616. [CrossRef]
21. Stirling, A.; Bernasconi, M.; Parrinello, M. Ab initio simulation of water interaction with the (100) surface of pyrite. *J. Chem. Phys.* **2003**, *118*, 8917–8926. [CrossRef]
22. Rai, B.; Sathish, P.; Malhotra, C.P.; Pradip, A.; Ayappa, K.G. Molecular dynamic simulations of self-assembled alkylthiolate monolayers on an Au (111) surface. *Langmuir* **2004**, *20*, 3138–3144. [CrossRef] [PubMed]
23. Humphrey, W.; Dalke, A.; Schulten, K. VMD: Visual molecular dynamics. *J. Mol. Graph.* **1996**, *14*, 33–38. [CrossRef]
24. Liu, W.; McDonald, I.; Luther, W.; Wang, X.; Miller, J.D. Bastnaesite flotation chemistry issues associated with alkyl phosphate collectors. *Miner. Eng.* **2018**, *127*, 286–295. [CrossRef]
25. Mackrodt, W.C. Atomistic simulation of the surfaces of oxides. *J. Chem. Soc. Faraday Trans.* **1989**, *85*, 541–554. [CrossRef]
26. Hutter, J.; Iannuzzi, M.; Schiffmann, F.; VandeVondele, J. CP2K: Atomistic simulations of condensed matter systems. *Wiley Interdiscip. Rev. Comput. Mol. Sci.* **2014**, *4*, 15–25. [CrossRef]
27. VandeVondele, J.; Hutter, J. Gaussian basis sets for accurate calculations on molecular systems in gas and condensed phases. *J. Chem. Phys.* **2007**, *127*, 114105. [CrossRef]
28. Perdew, J.P.; Burke, K.; Ernzerhof, M. Generalized gradient approximation made simple. *Phys. Rev. Lett.* **1996**, *77*, 3865. [CrossRef]
29. Jin, J.; Miller, J.D.; Dang, L.X.; Wick, C.D. Effect of surface oxidation on interfacial water structure at a pyrite (100) surface as studied by molecular dynamics simulation. *Int. J. Miner. Process.* **2015**, *139*, 64–76. [CrossRef]
30. Du, H.; Miller, J.D. Interfacial water structure and surface charge of selected alkali chloride salt crystals in saturated solu-tions: A molecular dynamics modeling study. *J. Phys. Chem. C.* **2007**, *111*, 10013–10022. [CrossRef]
31. Hu, Y.; Wu, B.; Xu, Z.; Yang, Z.; Yang, X. Solvation structure and dynamics for passivated Au nanoparticle in supercritical CO_2: A molecular dynamic simulation. *J. Colloid Interface Sci.* **2011**, *353*, 22–29. [CrossRef] [PubMed]
32. Rappé, A.K.; Casewit, C.J.; Colwell, K.S.; Goddard, W.A., III; Skiff, W.M. UFF, a full periodic table force field for molecular mechanics and molecular dynamics simulations. *J. Am. Chem. Soc.* **1992**, *114*, 10024–10035. [CrossRef]
33. Xu, Y.; Liu, Y.; Liu, G. Molecular dynamics simulation of water molecules adsorbed at muscovite (001) surface. *CIESC J.* **2014**, *65*, 4814–4822.
34. Yan, D.S. Hariyasa, Selective flotation of pyrite and gold tellurides. *Miner. Eng.* **1997**, *10*, 327–337. [CrossRef]
35. Fleming, S.D. Metals Recovery by Flotation. U.S. Patent US4946585, 18 September 1989.
36. Albright, T.A.; Burdett, J.K.; Whangbo, M. *Orbital Interactions in Chemistry*; John Wiley & Sons: Hoboken, NJ, USA, 2013.
37. Momany, F.A. Determination of partial atomic charges from ab initio molecular electrostatic potentials. Application to formamide, methanol, and formic acid. *J. Phys. Chem.* **1978**, *82*, 592–601. [CrossRef]
38. Besler, B.H.; Merz, K.M.; Kollman, P.A. Atomic charges derived from semiempirical methods. *J. Comput. Chem.* **1990**, *11*, 431–439. [CrossRef]
39. Williams, D.E. Net atomic charge and multipole models for the ab initio molecular electric potential. *Rev. Comput. Chem.* **2007**, *2*, 219–271.
40. Chen, J.; Chen, Y.; Li, Y. DFT calculation of amine cation collectors for zinc oxide flotation. *J. Guangxi Univ.* **2009**, *34*, 67–72.
41. Moncayo-Riascos, I.; Hoyos, B.A. Effect of collector molecular structure on the wettability of gold for froth flotation. *Appl. Surf. Sci.* **2017**, *420*, 691–699. [CrossRef]
42. Zhang, K. Spectroelectrochemical Investigations of the Interaction of Flotation Reagents with Gold Surfaces. Ph.D. Thesis, School of Natural Sciences, Griffith University, Brisbane, Australia, 2016.
43. Chen, J.; Lan, L.; Chen, Y. Computational simulation of adsorption and thermodynamic study of xanthate, dithiophosphate and dithiocarbamate on galena and pyrite surfaces. *Miner. Eng.* **2013**, *46–47*, 136–143. [CrossRef]
44. Yu, C.; Guan, J.; Chen, K.; Bae, S.C.; Granick, S. Single-molecule observation of long jumps in polymer adsorption. *ACS Nano* **2013**, *7*, 9735–9742. [CrossRef] [PubMed]
45. Monte, M.B.M.; Lins, F.F.; Oliveira, J.F. Selective flotation of gold from pyrite under oxidizing conditions. *Int. J. Miner. Process.* **1997**, *51*, 255–267. [CrossRef]